TASK QUARTERLY 7 No 3 (2003), 375–387

A TURBULENT HEAT FLUX TWO–EQUATION $\overline{\theta'^2}$–ε_θ CLOSURE BASED ON THE $V2F$ TURBULENCE MODEL

MICHAŁ KARCZ AND JANUSZ BADUR

Institute of Fluid-Flow Machinery, Polish Academy of Sciences,
Thermo-Chemical Power Department,
Fiszera 14, 80-952 Gdansk, Poland
{*mkarcz,jb*}*@imp.gda.pl*

(Received 3 January 2003; revised manuscript received 5 March 2003)

Abstract: The paper deals with the proposition of a two-equation turbulent heat flux closure without any damping function. The model has been based on Durbin's $V2F$ dynamic turbulence closure and the Deng-Wu-Xi thermal turbulence model. Both models have been implemented into the FLUENT code by a User Defined Function. Results of numerical computation have been compared with experimental data for developing a thermal field in a pipe by Nagano and DNS heat transfer prediction for a two-dimensional channel flow by Kasagi.

Keywords: turbulent heat transfer, turbulent Prandtl number, low-Reynolds-number models, Durbin's model of turbulence

1. Introduction

Turbulent heat flux modelling remains one of the unresolved problems of fluid dynamics. The usual way of modelling a turbulent heat flux in almost all CFD codes is simply by employing a constant or varying turbulent Prandtl number Pr_t that is a direct succesion of the Reynolds analogy between turbulent heat and momentum transfer. Such treatment has been sufficent and economical for the prediction of simple pipe or channel flows without separation. But this way could be no longer valid for flows in complicated, especially three-dimensional geometries [1], where more sofisticated models are necessary.

This paper has been focused on the two-equation $\overline{\theta'^2}$-ε_θ turbulent heat flux closure without any damping functions based on geometries characteristic for *low-Reynolds-number* models. As a consequence, a $V2F$ closure that works without damping functions has been employed for dynamic field modelling. The original $V2F$ model was originally proposed by Durbin in the early 1990's [2]. This model uses different velocity scales in turbulence diffusivity formulation than the turbulence kinetic energy that is usually employed in standard k-ε models. Instead of k, $\overline{v'^2}$, *i.e.* variance of the normal component of turbulent velocity, which could be viewed as

a kind of turbulent stress component, has been proposed. As a result, a new transport equation for $\overline{v'^2}$ has to be solved. Additionally, an equation for f, called the *elliptic-relaxation equation*, for the redistribution term of $\overline{v'^2}$ is necessary. This equation simply introduces a kinematic blocking effect of the wall and allows damping functions to be completly abandoned [2, 3]. Different versions of the original $V2F$ model have been widely implemented, tested and validated, especially for remarkable favorable pressure gradients and separation flows, where Durbin's proposition has been found to be a simple and reliable closure [3–8].

On the basis of $V2F$ and an additional two-equation $\overline{\theta'^2}$-ε_θ turbulent heat transfer model of Deng-Wu-Xi[1] [9], a new proposition for a turbulent heat flux closure is presented here. It assumes that $\overline{v'^2}$ should also be employed in turbulent heat diffusivity formulation: as a consequnce, damping functions are no longer necessary. Another modification has been necessary in the temperature-variance dissipation rate ε_θ transport equation, that allows one to correctly model near-wall changes. The constants of the model have been calibrated and validated on the basis of experiments by Nagano on the development of a thermal boundary layer in a pipe [10, 11] and DNS heat transfer data by Kasagi for two-dimensional channel flows [12].

2. Combined dynamic-thermal turbulence closure

Present CFD codes usually employ two-equation and full second-order closures of turbulent momentum flux. As has been mentioned above, the most popular way of computing a turbulent heat flux is simply by introducing the Reynolds analogy, which directly binds turbulent diffusivity of heat, α_t, with turbulent viscosity, ν_t, by an artificial turbulent Prandtl number, Pr_t. Common value of $\mathrm{Pr}_t = 1$ is a sufficient approximation for near-wall flows [13], but it is known that α_t should be at least represented as a function, not only dynamic but also thermal time scale which is the main assumption of two-equation $\overline{\theta'^2}$-ε_θ closures [9, 11, 13–15].

The concept of a combined $V2F$-DWX model has been established on the assumption that both turbulent momentum and heat transfer are controlled mainly by the turbulent velocity component normal to the wall [2, 3]. This velocity component, represented by $\overline{v'^2}$, is naturally damped in the vicinity of the wall, so it seems obvious to replace turbulent kinetic energy, k, together with damping functions f_μ and f_λ in both eddy diffusivity of momentum and heat formulations, respectively:

$$\nu_t \approx k^{\frac{1}{2}} L_m = C_\mu f_\mu k T_m = C_\mu \overline{v'^2} T_m, \tag{1}$$

$$\alpha_t \approx k^{\frac{1}{2}} L_t = C_\lambda f_\lambda k T_t = C_\lambda \overline{v'^2} T_t. \tag{2}$$

Turbulent time scale of turbulent viscosity T_m is usually defined as a relation of turbulent kinetic energy, k, and its dissipation rate, ε. Turbulent eddy diffusivity of heat, α_t, not only employs a dynamic time scale, k/ε, but also a thermal field time scale, $\overline{\theta'^2}/\varepsilon_\theta$:

$$T_t = \frac{k}{\varepsilon}^{l} \frac{\overline{\theta'^2}}{\varepsilon_\theta}^{m}, \qquad l + m = 1. \tag{3}$$

1. This model will be further called as a DWX for the sake of simplicity

As a result, α_t may be written as:

$$\alpha_t = C_\lambda \overline{v'^2} \frac{k}{\varepsilon}^l \frac{\overline{\theta'^2}}{\varepsilon_\theta}^m . \tag{4}$$

2.1. *V2F model*

There have been many implementations of the original Durbin [2] and modified versions of a $V2F$ closure. The modifications have been mainly connected with constants value and the way of establishing the time and length scales [5, 6]. The model employed in the present work has been based on such modified versions. A significant advantage of the $V2F$ turbulence closure seems to be the lack of damping functions of any kind.

A full set of transport equations of the $V2F$ model consists of:

- turbulent kinetic energy, k:

$$\frac{\partial}{\partial t}(\rho k) + \frac{\partial}{\partial x_j}(\rho v_j k) = \frac{\partial}{\partial x_j}\left[\left(\mu + \frac{\mu_t}{\sigma_k}\right)\frac{\partial k}{\partial x_j}\right] + P_k - \varepsilon; \tag{5}$$

- the dissipation rate of turbulent kinetic energy, ε:

$$\frac{\partial}{\partial t}(\rho \varepsilon) + \frac{\partial}{\partial x_j}(\rho v_j \varepsilon) = \frac{\partial}{\partial x_j}\left[\left(\mu + \frac{\mu_t}{\sigma_\varepsilon}\right)\frac{\partial \varepsilon}{\partial x_j}\right] + \frac{C_{\varepsilon 1} P_k - C_{\varepsilon 2}\varepsilon}{T}; \tag{6}$$

- turbulent stress normal component, $\overline{v'^2}$:

$$\frac{\partial}{\partial t}\left(\rho \overline{v'^2}\right) + \frac{\partial}{\partial x_j}\left(\rho v_j \overline{v'^2}\right) = \frac{\partial}{\partial x_j}\left[(\mu + \mu_t)\frac{\partial \overline{v'^2}}{\partial x_j}\right] + kf - \frac{\varepsilon}{k}\overline{v'^2}; \tag{7}$$

- elliptic relaxation-like equation of f:

$$f = L^2 \frac{\partial}{\partial x_j}\left(\frac{\partial f}{\partial x_j}\right) + \frac{C_1}{T}\left[\frac{2}{3} - \frac{\overline{v'^2}}{k}\right] + C_2 \frac{P_k}{k}. \tag{8}$$

The production of turbulent kinetic energy, P_k, has been usually based on the strain-rate tensor, d_{ij}:

$$P_k = 2\mu_t d_{ij} d_{ij}. \tag{9}$$

The turbulent length scale employed in Equation (8) has been computed from:

$$L = C_L \max\left[\frac{k^{\frac{3}{2}}}{\varepsilon}, C_\eta \left(\frac{\nu^3}{\varepsilon}\right)^{\frac{1}{4}}\right]. \tag{10}$$

The turbulent time scale could be prescribed by analogy to the lenght scale:

$$T = \max\left[\frac{k}{\varepsilon}, 6\sqrt{\frac{\nu}{\varepsilon}}\right]. \tag{11}$$

Model constants:

$$C_\mu = 0.22, \quad C_1 = 0.4, \quad C_2 = 0.3, \quad C_L = 0.25, \quad C_\eta = 85, \quad C_{\varepsilon 2} = 1.9, \quad \sigma_\varepsilon = 1.3.$$

The additional parameter $C_{\varepsilon 1}$ needs to be computed from:

$$C_{\varepsilon 1} = 1.4\left(1 + 0.045\sqrt{k \Big/ \overline{v'^2}}\right). \tag{12}$$

The boundary conditions at the wall, for all parameters, are:

$$k_w = 0, \quad \varepsilon = \frac{2\nu k_1}{{y_1}^2}, \quad \overline{v'^2} = 0, \quad f_w = -\frac{20\nu^2 \overline{v'^2}}{\varepsilon_w {y_1}^4}. \tag{13}$$

2.2. $\overline{\theta'^2}$-ε_θ model

Extensive work in the area of two-equation closures of turbulent heat flux has been done by the group of Nagano *et al.* Succesful implementation of the $\overline{\theta'^2}$-ε_θ model was first presented in 1988 [16]. Since then, a number of modified versions of the $\overline{\theta'^2}$-ε_θ model have been published ([9, 14, 15, 17]). Such modelling requires two additional transport equations, *viz.* temperature variance, $\overline{\theta'^2}$, and its destruction (dissipation) rate, ε_θ. The exact transport equations of temperature variance and its dissipation rate are given by Speziale [18] and Deng *et al.* [9].

The modelling of $\overline{\theta'^2}$ seems to be simple and could be based on the gradient hipothesis for diffusion and production terms closures. However, the modelling of ε_θ is more difficult. In this work, the DWX model of Deng *et al.* has been employed. Evolution equations of $\overline{\theta'^2}$ and ε_θ for the original DWX version could be given in the following form:

- temperature variance $\overline{\theta'^2}$:

$$\frac{\partial}{\partial t}\left(\rho\overline{\theta'^2}\right) + \frac{\partial}{\partial x_j}\left(\rho v_j \overline{\theta'^2}\right) = \frac{\partial}{\partial x_j}\left[\left(\alpha + \frac{\alpha_t}{\sigma_{\overline{\theta'^2}}}\right)\frac{\partial \overline{\theta'^2}}{\partial x_j}\right] + 2P_\theta - 2\varepsilon_\theta \ , \tag{14}$$

- dissipation rate of temperature variance ε_θ:

$$\begin{aligned}\frac{\partial}{\partial t}\left(\rho\varepsilon_\theta\right) + \frac{\partial}{\partial x_j}\left(\rho v_j \varepsilon_\theta\right) = \frac{\partial}{\partial x_j}\left[\left(\alpha + \frac{\alpha_t}{\sigma_{\varepsilon_\theta}}\right)\frac{\partial \varepsilon_\theta}{\partial x_j}\right] + \\ + C_{p1} f_{p1} \sqrt{\varepsilon\varepsilon_\theta / \left(k\overline{\theta'^2}\right)} P_\theta - C_{d1} f_{d1} \varepsilon_\theta \varepsilon_\theta / \overline{\theta'^2} - C_{d2} f_{d2} \varepsilon\varepsilon_\theta / \overline{\theta'^2} \ .\end{aligned} \tag{15}$$

The production rate of temperature variance, P_θ, could be found from the temperature gradients:

$$P_\theta = \alpha_t \frac{\partial^2 T}{\partial x_j \partial x_j}. \tag{16}$$

It is characteristic for the DWX closure that the production term of ε_θ is modeled only using the production rate of temperature variance and a mixed dynamic-thermal time scale. As has been mentioned above, a new formula for turbulent diffusivity of heat has been proposed, Equation (4). It now consists of the new velocity scale, $\overline{v'^2}$, and the mixed time scale. For the present analysis, two sets of new constants have been proposed for version 1 and 2, respectively.

The near-wall changes of the $C_\lambda f_\lambda k$ in DWX eddy diffusivity of heat α_t formulation, and its modified version $C_\lambda \overline{v'^2}$ are presented in Figure 1.

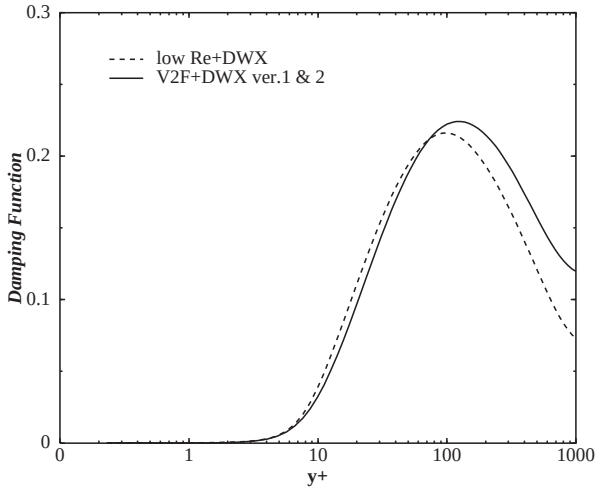

Figure 1. Diffusivity damping function, $C_\lambda f_\lambda k$, of the original DWX model and a new proposition, $C_\lambda \overline{v'^2}$, of versions 1 and 2

Version 1 of the implemented DWX model consists of:

$$C_\lambda = 0.23, \quad C_{p1} = 2.75, \quad C_{d1} = 2.1, \quad C_{d2} = 0.9,$$

$$f_\lambda = f_{p1} = f_{d1} = f_{d2} = 1, \quad l = 1.5, \quad m = -0.5, \quad \sigma_{\varepsilon_\theta} = 1.0, \quad \sigma_{\overline{\theta'^2}} = 1.0$$

Version 2 of the DWX model uses new damping-like function f_{d2} in the second dissipation term of ε_θ. The near-wall changes of the original and new f_{d2} are presented in Figure 2:

$$C_\lambda = 0.28, \quad C_{p1} = 2.6, \quad C_{d1} = 2.0, \quad C_{d2} = 1.5,$$

$$f_\lambda = f_{p1} = f_{d1} = 1, \quad f_{d2} = \sqrt{\overline{v'^2}/k}, \quad l = 0.5, \quad m = 0.5, \quad \sigma_{\varepsilon_\theta} = 1.0, \quad \sigma_{\overline{\theta'^2}} = 1.0$$

The boundary conditions on the impermeable walls have been assumed, for both versions of the model, to be identical to the original Deng's *et al.* proposition [9]:

$$\overline{\theta'^2} = 0, \quad \varepsilon_\theta = \alpha \frac{\overline{\theta_1'^2}}{\overline{y_1^2}}. \tag{17}$$

3. Numerical calculations

The problem of the thermal boundary layer developing in a pipe has been first investigated with the described models. The experiment of Nagano and Hishida seems to be a good test for validation of a new closure.

Detailed description of the experimental stand and results are given by [10] and [11]. In this experiment, velocity and temperature fluctuations in the thermal boundary layer developing in a turbulent pipe flow of air with uniform wall temperature have been measured. The diameter of pipe was $d = 45.68$mm. The heating section began at a distance of $127d$ from the inlet of the pipe. So great a distance was sufficient to make the turbulent flow of air in the pipe fully developed hydrodynamically. The length of the heating section was $40d$. Uniform wall temperature $\theta_w = 373$K was maintained with saturated steam at atmospheric pressure. Measurements were made at six cross-sections at x/d from the beginning of the heating section.

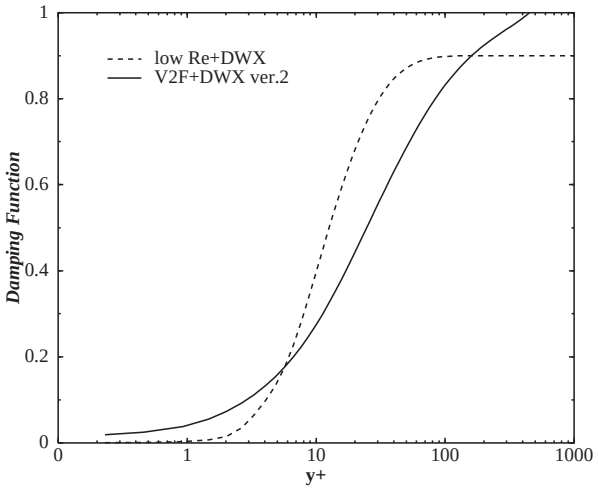

Figure 2. Diffusivity damping function, f_{d2}, of the original DWX model and a new proposition, $\sqrt{\frac{\overline{v'^2}}{k}}$, of version 2

The numerical calculations were carried out with the aid of the FLUENT package [19]. In the present analysis, three models have been employed, *viz.* the original DWX formulation and its modified versions 1 and 2. All mentioned models and the $V2F$ closure have been implemented into the solver by the subroutines. The original DWX formulation required a *low-Reynolds-number* k-ε model Abe-Kondoh-Nagano [20] to be activated.

The axisymmetric numerical domain was discretized with a structural grid of finite volumes with exponential distribution of vertex to the wall. The numerical mesh consisted of 80 finite volumes in the streamwise direction. It allowed us to obtain a nondimensional parameter y^+ in the limit of 0.1 at the wall. The QUICK scheme was used to discretize the governing equations. The pressure-velocity coupling was resolved with the aid of the SIMPLEC method.

Air flow was treated as a compressible ideal gas. Molecular conductivity was modeled by a polynomial function of temperature:

$$\lambda = 1.5207 \cdot 10^{-11}\theta^3 - 4.8574 \cdot 10^{-8}\theta^2 + 1.0184 \cdot 10^{-4}\theta - 3.9333 \cdot 10^{-3}. \qquad (18)$$

Molecular viscosity was also modeled as a function of temperature, with the aid of the Sutherland law.

The results of calculations have been presented here for three cross-sections of the heating section, namely a) $x/d = 1$, b) 5.89 and c) 39.89. The numerical results have been compared with the experimental data for normalized temperature, θ^+ (Figure 3), turbulent heat flux, $(-\overline{v'\theta'})^+$ (Figure 4), temperature variance, $\left(\frac{\overline{\theta'^2}}{2}\right)^+$ (Figure 5), and production of temperature variance (Figure 6). Additionally, changes of the measured and computed turbulent Prandtl number in the fully developed thermal boundary layer at $x/d = 39.89$ have been presented in Figure 7.

As can be seen in Figure 3, all the implemented models have predicted changes of temperature in the developing thermal region quite well. Likewise, the turbulent heat flux in Figure 4 has been predicted almost identically. Differences are visible only

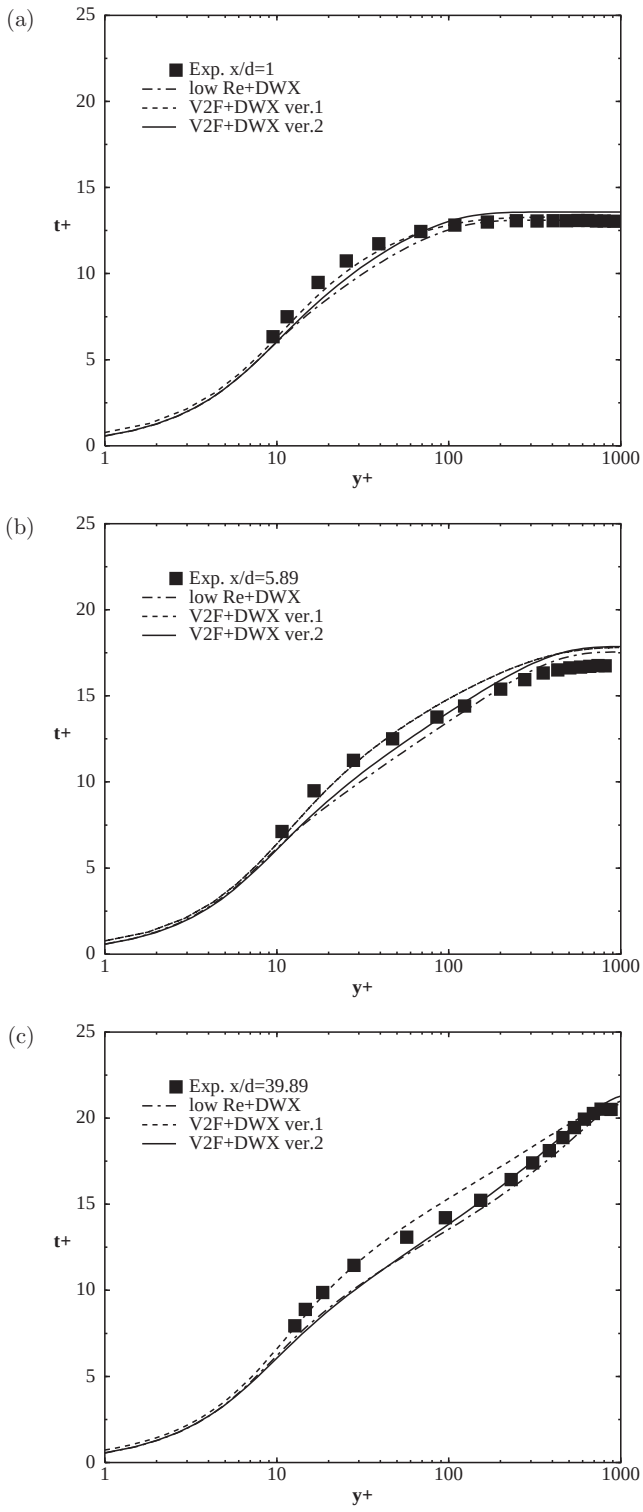

Figure 3. Normalized temperature, θ^+

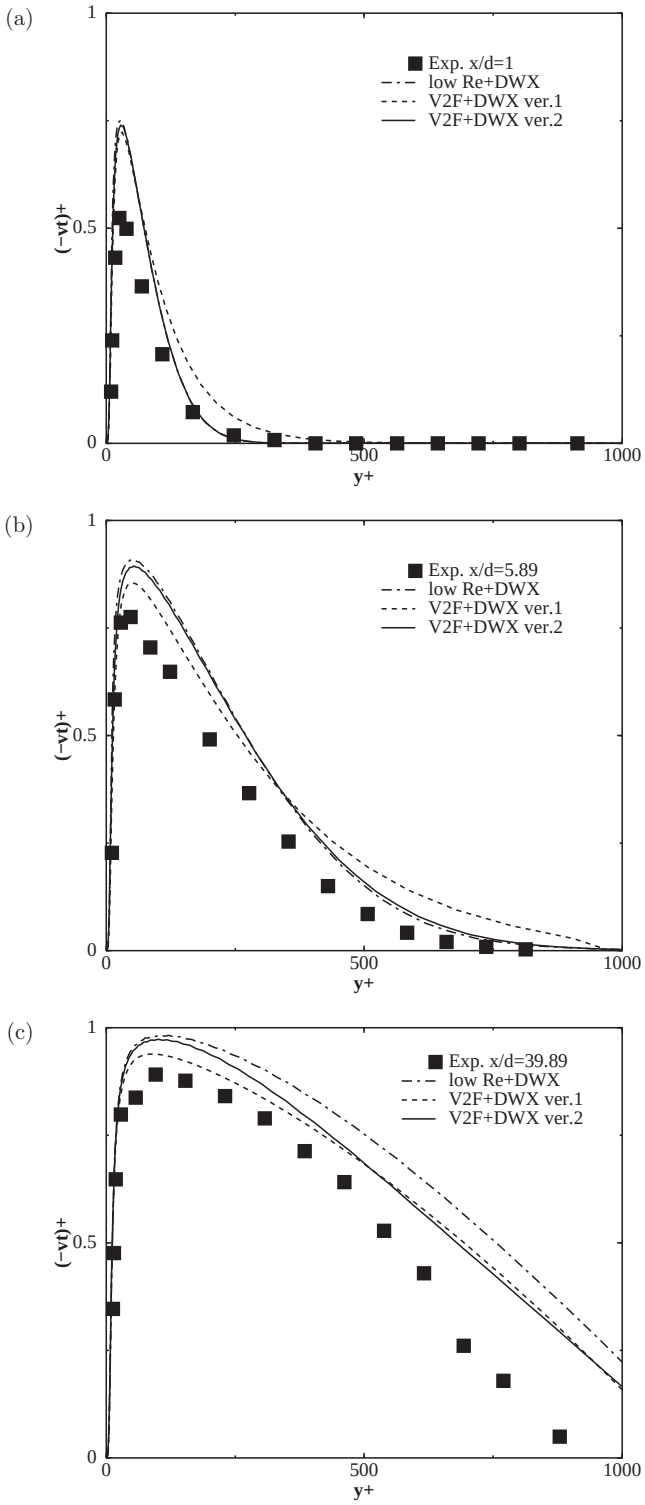

Figure 4. Normalized turbulent heat flux, $(-\overline{v'\theta'})^+$

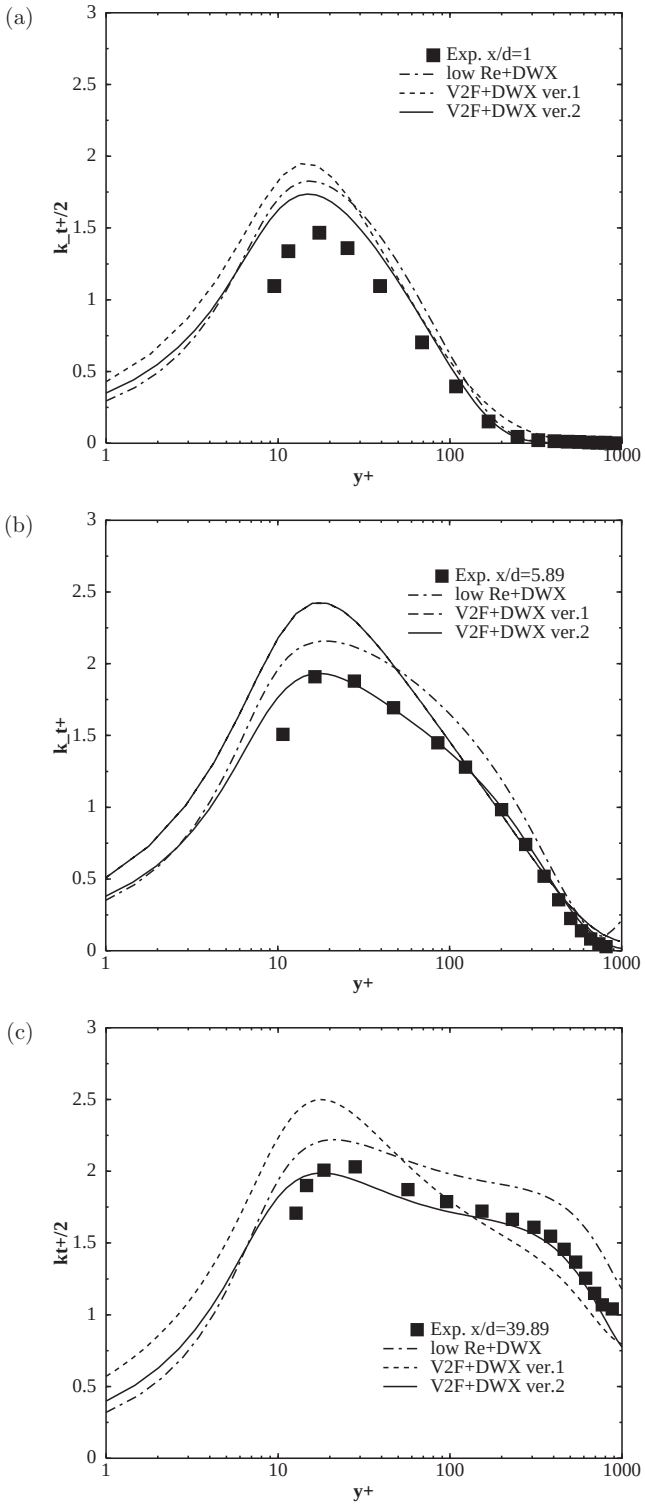

Figure 5. Normalized temperature variance, $\left(\frac{\overline{\theta'^2}}{2}\right)^+$

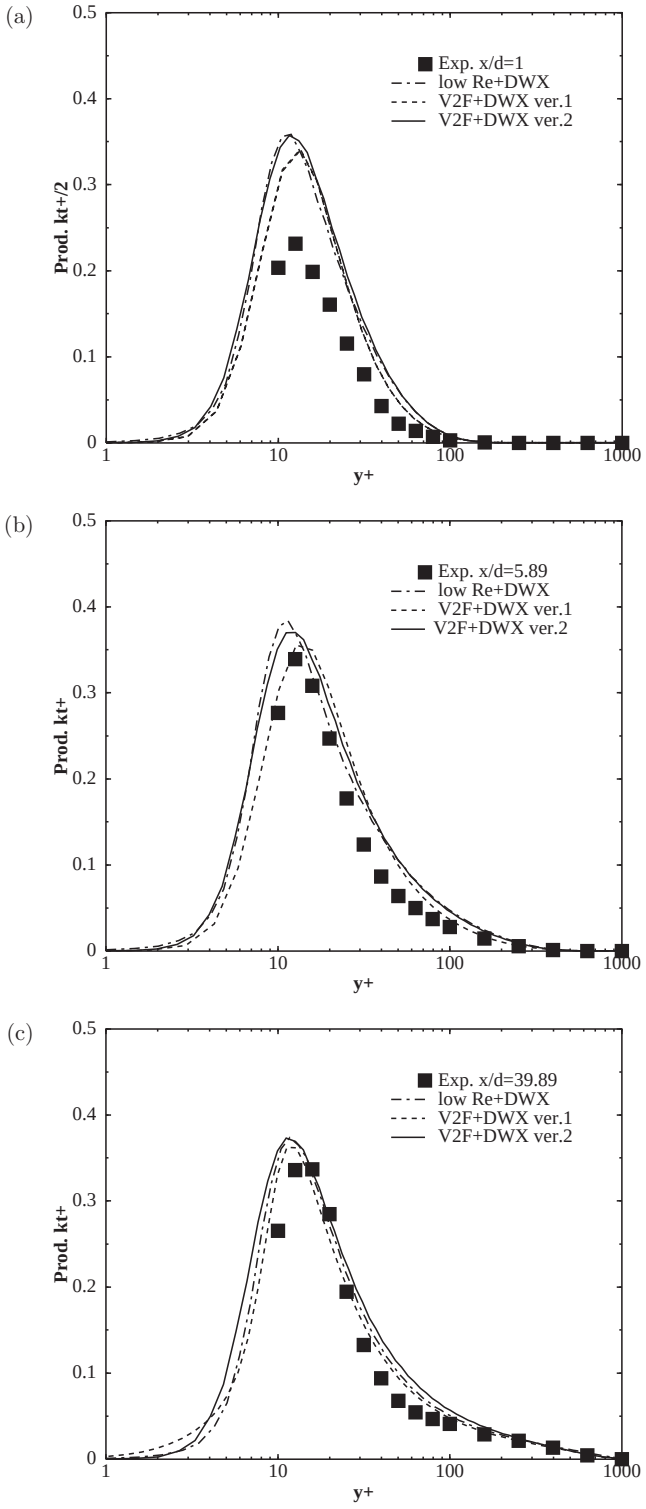

Figure 6. Normalized production of temperature variance, $\left(\frac{\overline{\theta'^2}}{2}\right)^+$

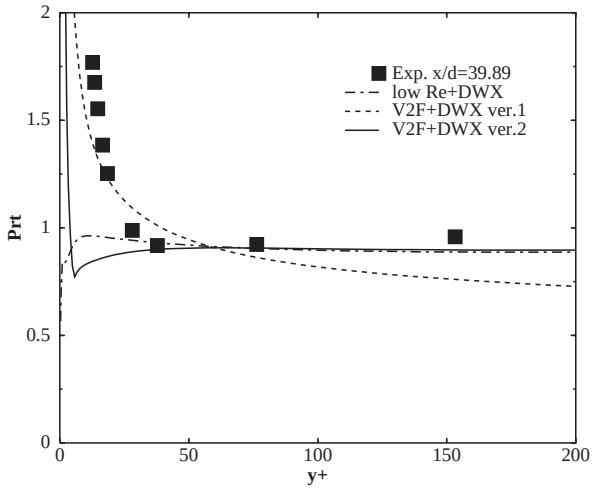

Figure 7. Turbulent Prandtl number, Pr_t

for the undeveloped region at the beginning of the heating section. A similar trend has been observed for normalized temperature variance (Figure 5). In this case, the best results have been obtained with the original DWX formulation and its modified version 2, and it seems that version 2 has predicted changes of $\left(\overline{\theta'^2}\right)^+$ slightly better. The worst results have been obtained with version 1 of the modified model, for the all of cross-sections: maximum values of $\left(\overline{\theta'^2}\right)^+$ have been overestimated by about 20%. Results for the production rate of temperature variance are close for all the employed models (Figure 6). Different trends have been revealed for changes of the turbulent Prandtl number in Figure 7. Close to the wall, $y^+ < 50$, the best agreement has been achieved with version 1 of DWX, but its prediction has failed in the core, where Pr_t chopped to too low values. The original DWX model and its version 2 have predicted the value of the turbulent Prandtl number very well far from the wall, but close to the wall Pr_t has behaved in the opposite manner. The original DWX formulation has given a particularly wrong prediction of Pr_t changes near the heating surface.

Additionally, all the implemtented models have also been compared with DNS predictions of fully developed turbulent channel flows with heat transfer [12]. DNS data of turbulent flows have been a major source of information on near-wall behavior. Real experiments are usually limited by technological or economical constraints of detailed measurements in the thin boundary layer, so, in such situations, DNS calculations are very helpful. There is also a problem with DNS databases, in that they are usually limited to simple channel geometry and to low Reynolds number flows.

The most interesting aspect of the present analysis has been comparing the budgets of temperature variance, $\overline{\theta'^2}$, in Figure 8 and its dissipation rate, ε_θ in Figure 9. The particular diagrams shown in those figures have been made for results of (a) DNS, (b) the original DWX formulation, (c) version 1 and (d) version 2 of the DWX model. As it could be clearly seen in Figure 8, the budgets of $\overline{\theta'^2}$ for all the implemtented models have been very close to DNS predictions. The only differences have been visible for the near-wall behavior of the dissipation rate, but this has been common to all models. Obvious differences have been revealed in Figure 9.

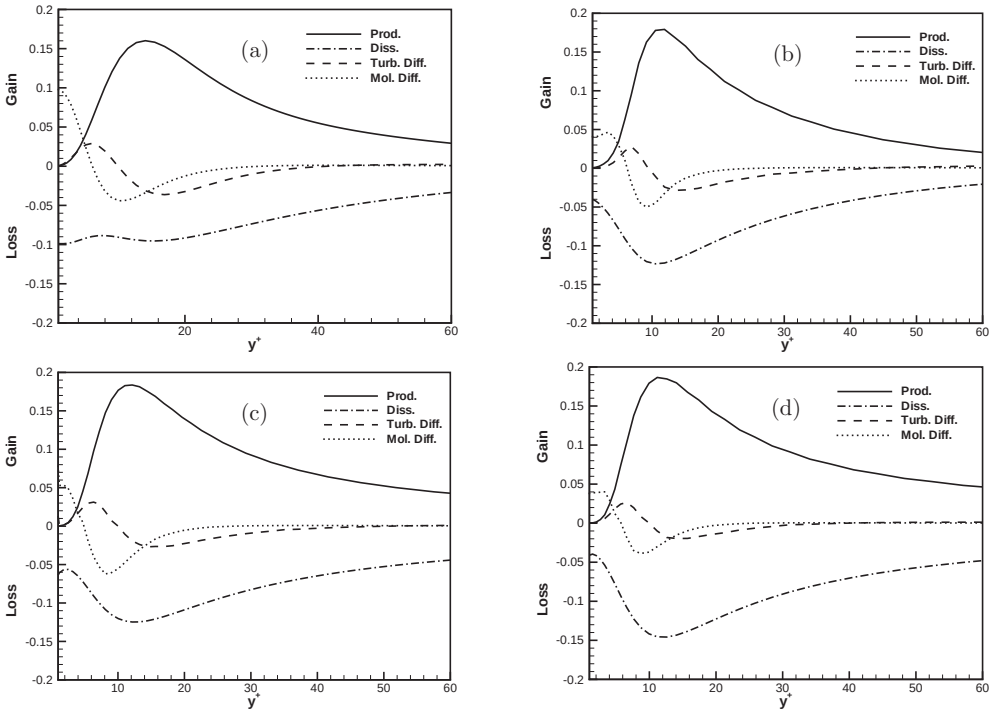

Figure 8. Budget of the normalized temperature variance $\overline{\theta^2}$: (a) DNS, (b) the original DWX formulation, (c) version 1 and (d) version 2 of the DWX model

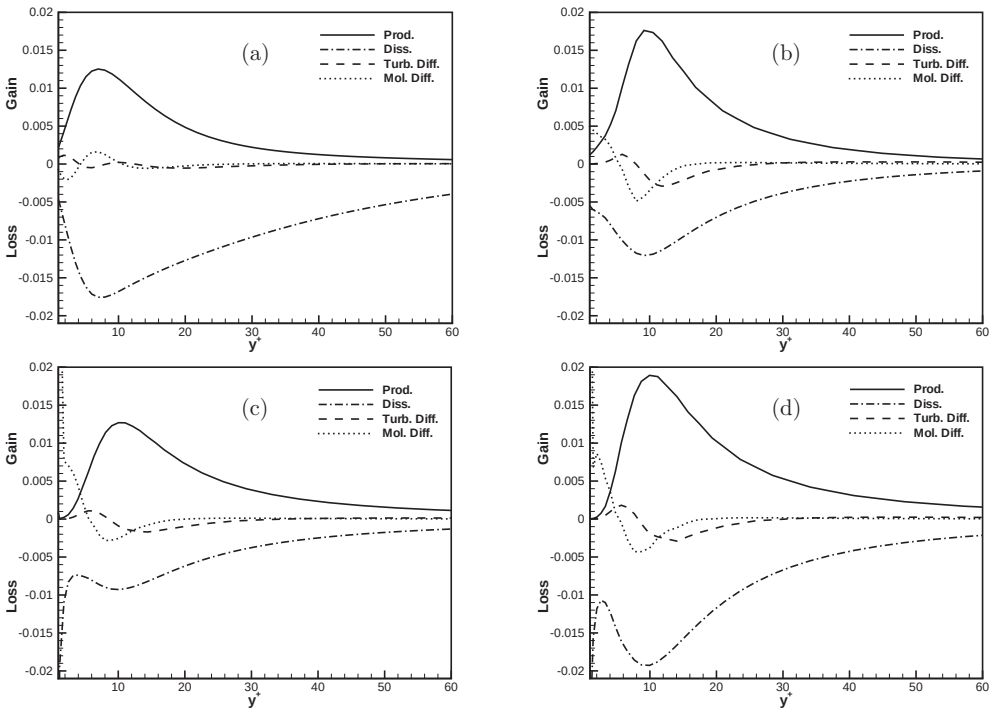

Figure 9. Budget of the normalized destruction rate of temperature variance ε_θ: (a) DNS, (b) the original DWX formulation, (c) version 1 and (d) version 2 of the DWX model

DNS results have indicated that, in the near-wall region, dissipation of ε_θ prevails over its production. Only version 2 of the DWX model has yielded similar behavior, even though the level of production and dissipation has been slightly higher. Both the original and the modified version 1 of DWX formulations have predicted too low dissipation levels.

4. Conclusions

Three models have been employed in the present analysis. Two of them, namely version 1 and 2, have been new propositions that could work with the $V2F$ turbulence closure. The new formulation of the eddy diffusivity of heat with velocity scale $\overline{v'^2}$ instead of k seems to be a correct assumption in view of the results presented in this paper. The best agreement with experimental and DNS data could be obtained with version 2 of the DWX model. This has been directly connected with the employment of a damping-like function in the ε_θ transport equation.

Acknowledgements

This research has been supported by the State Committee of Scientific Research (KBN) under the contract PB 1733/T10/2000/19.

References

[1] Kays W M 1994 *ASME J. Heat Transfer* **116** 284
[2] Durbin P A 1995 *AIAA J.* **33** 659
[3] Manceau R 2000 *Proc. European Congress on Computational Methods in Applied Sciences and Engineering, ECCOMAS 2000*, Barcelona, Spain, pp. 1–20
[4] Iaccarino G 2001 *ASME J. Engng.* **123** 819
[5] Kalitzin G 1999 *Annual Research Briefs*, Center for Turbulence Research of Stanford University, pp. 289–300
[6] Kalitzin G 1998 *Annual Research Briefs*, Center for Turbulence Research of Stanford University, pp. 171–184
[7] Manceau R, Parneix S and Laurence D 2000 *Int. J. Heat and Fluid Flow* **21** 320
[8] Karcz M 2002 *Internal Report of IFFM PAS-ci*, Gdansk, Poland **2366/02** 1 (in Polish)
[9] Deng B, Wu W and Xi S 2001 *Int. J. Heat and Mass Transfer* **44** 691
[10] Hishida M and Nagano Y 1979 *ASME J. Heat Transfer* **101** 15
[11] Nagano Y and Tagawa M 1988 *J. Fluid Mechanics* **196** 157
[12] Kasagi N, Tomita Y and Kuroda A 1992 *ASME J. Heat Transfer* **114** 598
[13] Pozorski J 2000 *Scientific Bulletin of IFFM PAS-ci*, Gdansk, Poland **515/1474/2000** 1 (in Polish)
[14] Abe K, Kondoh T and Nagano Y 1995 *Int. J. Heat and Mass Transfer* **38** 1467
[15] Nagano Y 1999 *Proc. Conf. Closure Strategies for Modelling Turbulent and Transitional Flows*, Cambridge, United Kingdom, pp. 1–52
[16] Nagano Y and Kim C 1988 *ASME J. Heat Transfer* **110** 583
[17] Youssef M S, Nagano Y and Tagawa M 1992 *Int. J. Heat and Mass Transfer* **35** 3095
[18] Speziale C G and So R M C 1998 *Int. J. Heat and Fluid Flow* **21** 320
[19] 1997–2002 *FLUENT User's Guide*, Fluent Inc., Lebanon, USA
[20] Abe K, Kondoh T and Nagano Y 1994 *Int. J. Heat and Mass Transfer* **37** 139